

# PARTIAL OUTER CONVEXIFICATION FOR TRAFFIC LIGHT OPTIMIZATION IN ROAD NETWORKS

S. GÖTTLICH\*, A. POTSCHKA†, AND U. ZIEGLER\*

**Abstract.** We consider the problem of computing optimal traffic light programs for urban road intersections using traffic flow conservation laws on networks. Based on a Partial Outer Convexification approach, which has been successfully applied in the area of mixed-integer optimal control for systems of ordinary or differential algebraic equations, we develop a computationally tractable two-stage solution heuristic. The two-stage approach consists of the solution of a (smoothed) Nonlinear Programming Problem with dynamic constraints and a reconstruction Mixed-Integer Linear Program without dynamic constraints. The two-stage approach is founded on a discrete approximation lemma for Partial Outer Convexification, whose grid independence properties for (smoothed) conservation laws we investigate. We use the two-stage approach to compute traffic light programs for two scenarios on different discretizations and demonstrate that the solution candidates cannot be improved in a reasonable amount of time by global state-of-the-art Mixed-Integer Nonlinear Programming Solvers. In addition, the two-stage solution candidates are better than results obtained by global optimization of piecewise linearized traffic flow models, in addition to being computed faster.

**Key words.** Partial outer convexification, traffic networks, discretized conservation laws, optimization, mixed-integer programming

**AMS subject classifications.** 35L65, 49J20, 90C11, 90C35

**1. Introduction.** With their seminal papers [18, 19] in the 1950s on time-dependent models for traffic flow with continuous densities instead of individual cars, Lighthill and Richards have established a new area of mathematical research in traffic modeling. The area is still highly active, e.g., for the case of traffic intersections (see, e.g., [3, 7]), which constitute a building block of larger road networks. Our goal in this article is to devise efficient heuristics to approximately solve the problem of optimal traffic light settings for road networks. We base our work on the model and scenarios presented in [9] and refer the reader to the discussion therein for further references regarding the wide variety of different approaches for traffic light control.

The resulting mathematical optimization problems, which we elaborate in full detail in §2, can be described as nonlinear mixed-integer optimal control problems constrained by scalar hyperbolic conservation laws on networks using boundary control. These problems are extremely challenging for several reasons: First of all, the problems are infinite dimensional in nature and must be discretized appropriately. Special care has to be exercised for the discretization of the scalar conservation laws in order to guarantee well-posedness and, on the discrete level, consistency and stability. Due to their combination of discrete and continuous variables, they are hybrid in nature and on fine discretizations, the combinatorial complexity of the feasible set is tremendous. In addition, the nonlinearities require sophisticated theoretical and numerical methods.

For nonlinear mixed-integer optimal control problems constrained by ordinary or differential algebraic equations, Sager et al. [20] have pioneered a Partial Outer Convexification (POC) approach which yields strong theoretical results, including existence of feasible points with arbitrarily small integer optimality gap. The proofs are

---

\*University of Mannheim, School of Business Informatics and Mathematics, 68131 Mannheim, GERMANY

†Heidelberg University, Interdisciplinary Center for Scientific Computing, Im Neuenheimer Feld 368, 69120 Heidelberg, GERMANY, email: potschka@iwr.uni-heidelberg.de. Support within the ERC Advanced Investigator Grant MOBOCON (291 458) is gratefully acknowledged.

constructive and lend themselves directly to the formulation of a numerical method, which outperforms conventional branch and bound methods from Mixed-Integer Non-linear Programming (MINLP) by several orders of magnitude on a test example, see [8, 16]. In [11], Hante and Sager have extended the POC approach to mixed-integer optimal control problems constrained by semilinear evolution equations. Due to certain smoothness assumptions on the solution, these results cover Partial Differential Equation (PDE) constraints of parabolic type. Recently, Hante [10] developed a POC theory for the case of mixed-integer optimal control problems constrained by first order semilinear hyperbolic systems in one space dimension with distributed control. His problem setting is close to our setting but so far the generalization of his proof techniques to the case of boundary control seems to be out of reach at least, if not impossible at all.

The efficiency of the POC approach lies in its exploitation of the special point-wise nature of causality that the physical time imposes on the mixed-integer control decisions. For realistic solutions in traffic light control, however, we need to satisfy additional combinatorial constraints that tightly couple control decisions over certain time intervals, e.g., maximum red light and minimum green light phases. These constraints are only marginally addressed in [10], with a direct reference to the Combinatorial Integer Approximation Problem (CIAP) introduced by Sager et al. [21]. In the presence of such coupling combinatorial constraints, the integer optimality gap in the POC approach cannot be reduced to arbitrarily small values anymore.

In this article, we investigate how the heuristics based on the POC/CIAP approach compare in terms of optimality and computational efficiency with existing MINLP methods and linearization plus Mixed-Integer Linear Programming (MILP) methods. To this end, we first discretize the traffic light optimization problem appropriately and present a smoothing argument, which allows to establish a time grid independent discrete POC approximation lemma. The constants we obtain are, however, not independent of the spatial discretization grid.

**2. Problem formulation.** We first describe the road network traffic flow equations, which appear as constraints in the dynamic optimization problem to be described subsequently.

**2.1. Traffic flow on road networks.** Coclite et al. [3] proposed a model for traffic flow on road networks with one junction. A generalization to multi-junction networks with traffic lights is straightforward (cf. [9]): We model the road network as a directed graph  $(V, E)$  with vertices  $V = \{1, \dots, n_V\}$  as junctions and edges  $E = \{1, \dots, n_E\}$  as uni-directional roads and denote the sets of incoming and outgoing roads of junctions  $v \in V$  as  $\delta_v^{\text{in}} \subset E$  and  $\delta_v^{\text{out}} \subset E$ . We partition the network vertices into the three sets of incoming, outgoing, and inner junctions

$$V^{\text{in}} = \{v \in V \mid \delta_v^{\text{in}} = \emptyset\}, \quad V^{\text{out}} = \{v \in V \mid \delta_v^{\text{out}} = \emptyset\}, \quad V^{\text{io}} = V \setminus \{V^{\text{in}} \cup V^{\text{out}}\}.$$

In addition, we denote the sets of incoming and outgoing roads of the network by

$$E^{\text{in}} = \{i \in E \mid \exists v \in V^{\text{in}} : i \in \delta_v^{\text{out}}\} \quad \text{and} \quad E^{\text{out}} = \{i \in E \mid \exists v \in V^{\text{out}} : i \in \delta_v^{\text{in}}\}.$$

Each road  $i \in E$  has a given length  $L_i > 0$ . On the time horizon  $[0, T]$  the road traffic densities  $\rho_i(t, x) \in [0, \rho^{\text{max}}]$ , which we normalize to  $\rho^{\text{max}} = 1$  for the sake of simplicity and without loss of generality, satisfy for all  $i \in E$  the one-dimensional hyperbolic conservation law

$$\partial_t \rho_i + \partial_x f(\rho_i) = 0 \quad \text{on } [0, T] \times [0, L_i], \quad (2.1)$$

where  $f : [0, 1] \rightarrow \mathbb{R}$  is a non-negative nonlinear continuous and piecewise twice continuously differentiable flow function with  $f(0) = f(1) = 0$ , a unique strict maximum at some  $\rho^* \in (0, 1)$ , and strict monotonicity on the intervals  $(0, \rho^*)$  and  $(\rho^*, 1)$ . These assumptions guarantee the existence of a continuous function  $\tau : [0, 1] \rightarrow [0, 1]$  with the properties  $\tau(\rho) \neq \rho$  and  $f(\rho) = f(\tau(\rho))$  for all  $\rho \in [0, 1] \setminus \rho^*$ .

The densities must satisfy the given initial conditions

$$\rho_i(0, x) = \rho_i^0(x) \quad \text{for all } x \in [0, L_i], i \in E. \quad (2.2)$$

The prescribed spatial boundary conditions depend on the road network topology and on the current traffic light setting. On incoming roads of the network, we prescribe inhomogeneous Dirichlet inflow data

$$\rho_i(t, 0) = \rho_i^{\text{in}}(t) \quad \text{for all } t \in [0, T], i \in E^{\text{in}}. \quad (2.3)$$

On outgoing roads  $i \in E^{\text{out}}$ , free outflow is guaranteed by the omission of boundary conditions at  $x = L_i$  for all  $t \in [0, T]$ . We assume that all roads  $i \in E \setminus E^{\text{out}}$  have a traffic light at  $x = L_i$  whose setting at time  $t \in [0, T]$  is denoted by  $A_i(t) \in \{0, 1\}$ , where 0 means red/stop and 1 means green/go. At red lights, a no flow condition must hold

$$f(\rho_i(t, L_i)) = 0 \quad \text{for all } t \in [0, T], i \in E \setminus E^{\text{out}} \text{ with } A_i(t) = 0. \quad (2.4)$$

For the sake of well-posedness of the Riemann problems at the inner junctions (see [3]) we need to require for all  $t \in [0, T]$  and each inner vertex  $v \in V^{\text{io}}$  the following relations to describe admissible boundary densities  $\hat{\rho}_i(t)$ ,  $i \in \delta_v^{\text{in}}$ , and  $\bar{\rho}_i(t)$ ,  $i \in \delta_v^{\text{out}}$ , and their corresponding fluxes  $\hat{\gamma}_i(t)$ ,  $i \in \delta_v^{\text{in}}$ , and  $\bar{\gamma}_i(t)$ ,  $i \in \delta_v^{\text{out}}$ ,

$$\hat{\rho}_i(t) \in \begin{cases} \{\rho_i(t, L_i)\} \cup (\tau(\rho_i(t, L_i)), 1] & \text{if } \rho_i(t, L_i) \in [0, \rho^*], \\ [\rho^*, 1] & \text{otherwise,} \end{cases} \quad \text{for } i \in \delta_v^{\text{in}}, \quad (2.5a)$$

$$\bar{\rho}_i(t) \in \begin{cases} [0, \rho^*] & \text{if } \rho_i(t, 0) \in [0, \rho^*], \\ \{\rho_i(t, 0)\} \cup [0, \tau(\rho_i(t, 0))] & \text{otherwise,} \end{cases} \quad \text{for } i \in \delta_v^{\text{out}}, \quad (2.5b)$$

$$A_i(t)\hat{\gamma}_i(t) \leq \begin{cases} f(\rho_i(t, L_i)) & \text{if } \rho_i(t, L_i) \in [0, \rho^*], \\ f(\rho^*) & \text{otherwise,} \end{cases} \quad \text{for } i \in \delta_v^{\text{in}}, \quad (2.5c)$$

$$\bar{\gamma}_i(t) \leq \begin{cases} f(\rho^*) & \text{if } \rho_i(t, 0) \in [0, \rho^*], \\ f(\rho_i(t, 0)) & \text{otherwise,} \end{cases} \quad \text{for } i \in \delta_v^{\text{out}}. \quad (2.5d)$$

In contrast to the usual notation, we use  $A_i(t)\hat{\gamma}_i(t)$  in place of  $\hat{\gamma}_i(t)$  in order to make the usually implicit dependence of  $\hat{\gamma}_i(t)$  on  $A_i(t)$  explicit (cf. e.g., [9]), because this reformulation dramatically improves the performance of the solvers for the Stage I problem to be introduced in §5. Moreover, we require the Rankine-Hugoniot relation for the conservation of traffic

$$\sum_{j \in \delta_v^{\text{out}}} \bar{\gamma}_j(t) = \sum_{i \in \delta_v^{\text{in}}} A_i(t)\hat{\gamma}_i(t) \quad \text{for all } t \in [0, T], v \in V^{\text{io}}. \quad (2.6)$$

In order to guarantee unique solvability of the so far still underdetermined Riemann problems at inner junctions, we require the following two additional conditions (2.7)

and (2.8): We model the vehicles' turning preferences with an  $n_E \times n_E$  traffic distribution matrix, whose entries  $d_{ij} \in [0, 1]$  describe the fraction of traffic turning from road  $i$  into road  $j$  according to

$$\bar{\gamma}_j(t) = \sum_{i \in \delta_v^{\text{in}}} d_{ij} A_i(t) \hat{\gamma}_i(t) \quad \text{for all } t \in [0, T], j \in \delta_v^{\text{out}}, v \in V^{\text{io}}. \quad (2.7)$$

For consistency with (2.6), the matrix entries must satisfy

$$\sum_{j \in \delta_v^{\text{out}}} d_{ij} = 1 \quad \text{for all } i \in \delta_v^{\text{in}}, v \in V^{\text{io}}.$$

Finally, we assume that the traffic distributes itself at the inner junctions in a way that maximizes the junction traffic flows

$$\max \sum_{i \in \delta_v^{\text{in}}} \bar{\gamma}_i(t) \quad \text{for all } t \in [0, T], v \in V^{\text{io}}, \quad (2.8)$$

which, due to (2.6), is equivalent to maximizing the sum of the terms  $A_i(t) \hat{\gamma}_i(t)$  for  $i \in \delta_v^{\text{out}}, v \in V^{\text{io}}$ , as usually stated (cf. e.g., [9]). Equations (2.1)–(2.8) completely describe the traffic flow dynamics.

**2.2. Traffic light optimization.** For a given road network we want to determine traffic light programs that maximize the cumulative traffic flow within the network. In realistic situations, further combinatorial constraints must be respected, e.g., logical implications of light configurations to avoid colliding crosstraffic at junctions, but possibly also bounds on the minimum green light or maximum red light phase durations.

The traffic light optimization problem can be cast in the form

$$\max_{\substack{A_i: [0, T] \rightarrow \{0, 1\}, i \in E \setminus E^{\text{out}} \\ \rho_i: [0, T] \times [0, L_i] \rightarrow [0, 1], i \in E}} \sum_{i \in E} \int_0^T \int_0^{L_i} f(\rho_i(t, x)) dx dt + \sum_{i \in E \setminus E^{\text{in}}} \int_0^T \bar{\gamma}_i(t) dt, \quad (2.9)$$

subject to (2.1)–(2.8) and additional combinatorial constraints.

Another way of posing problem (2.9) makes use of a Disjunctive Programming viewpoint [2] and paves the way for the application of Partial Outer Convexification in §4. To this end, we enumerate all feasible traffic light configurations at a time  $t \in [0, T]$  in a set  $\Omega := \{a^1, \dots, a^{n_\Omega}\}$  of binary vectors  $a^j \in \{0, 1\}^{n_E}$  for  $j = 1, \dots, n_\Omega$ . The number  $n_\Omega$  of elements in  $\Omega$  is at most  $2^{n_E}$ . At this point, infeasible configurations with red lights at the end of outgoing roads or with violations of other time-independent logical implications can already be removed from  $\Omega$  so that  $n_\Omega \ll 2^{|E \setminus E^{\text{out}}|}$ , e.g.,  $n_\Omega = 16 \ll 2^8$  as in the large intersection example with eight traffic lights in §6. At each time  $t \in [0, T]$  exactly one traffic light configuration is active, which we denote by a binary function  $\omega: [0, T] \rightarrow \{0, 1\}^{n_\Omega}$  that satisfies for  $j = 1, \dots, n_\Omega$  the relation

$$\omega_j(t) = 1 \quad \Leftrightarrow \quad A_i(t) = a_i^j \quad \text{for all } i = 1, \dots, n_E.$$

The optimization problem (2.9) can now equivalently be stated as

$$\begin{aligned}
 & \max_{\substack{\omega: [0, T] \rightarrow \{0, 1\}^{n_\Omega} \\ \rho_i: [0, T] \times [0, L_i] \rightarrow [0, 1], i \in E}} \sum_{i \in E} \int_0^T \int_0^{L_i} f(\rho_i(t, x)) dx dt + \sum_{i \in E \setminus E^{\text{in}}} \int_0^T \bar{\gamma}_i(t) dt, \\
 & \text{subject to} \quad (2.1) - (2.8) \text{ without (2.4),} \\
 & \quad \bigvee_{s=1}^{n_\Omega} \left[ \begin{array}{l} \omega_s(t) = 1 \\ f(\rho_i(t, L_i)) = 0 \quad \forall i \in E : a_i^s = 0 \end{array} \right] \quad \text{for all } t \in [0, T], \\
 & \quad \text{and additional combinatorial constraints coupling over time,} \\
 & \quad (2.10)
 \end{aligned}$$

where the logical operator  $\bigvee_{s=1}^{n_\Omega}$  implies that exactly one of the  $n_\Omega$  logical terms in brackets is true at each time  $t \in [0, T]$ .

The main challenges of solving problems (2.9) and (2.10) are fourfold: First, the optimization variables and dynamic equations are temporally and spatially distributed on a complex network and must be discretized with care to properly capture the hyperbolic traffic dynamics, which include shock formations and rarefaction waves. Second, the resulting problems will be of large scale and thus require the use of sophisticated algorithms and computational machinery. Third, the problems contain binary decision variables and are thus of combinatorial nature. Fourth, the objective and constraints are nonlinear and nonconvex. Hence, efficient off-the-shelf methods from mixed-integer linear programming cannot be applied as such. All four challenges alone constitute highly active areas of current research. The combination of the four renders problems (2.9) and (2.10) especially hard.

**3. Discretization.** We want to approximate problem (2.10) with a finite dimensional optimization problem. To this end, we discretize for each road  $i \in E$  the traffic densities  $\rho_i$  on an equidistant cartesian grid with (for simplicity) uniform time steps  $\Delta t > 0$  and spatial mesh size of  $\Delta x^i > 0$  uniformly on each road. We assume that  $n_T = T/\Delta t$  and  $n_L^i = L_i/\Delta x^i$  are integer for all  $i \in E$  and set

$$\rho_{t,k}^i = \rho_i(t\Delta t, k\Delta x^i) \quad \text{for } i \in E, t = 0, \dots, n_T, k = 0, \dots, n_L^i.$$

We use the same staggered Lax-Friedrichs (sLxF) method as in [9] for the discretization of (2.1) (only the presentation chosen here differs slightly in order to facilitate the use within Partial Outer Convexification): To describe the traffic flow at the junctions regarding (2.5), we introduce for  $t = 0, \dots, n_T - 1$  the temporally distributed real variables

$$\hat{\gamma}_t^i, \hat{h}_t^i \text{ for } i \in E \setminus E^{\text{out}} \quad \text{and} \quad \bar{\gamma}_t^i, \bar{h}_t^i \text{ for } i \in E \setminus E^{\text{in}}.$$

For all  $t = 0, \dots, n_T$  the densities  $\rho_{t,k}^i$  for  $k \in \{-1, n_L^i + 1\}, i \in E$ , the variables  $\hat{\gamma}_t^i$  and  $\hat{h}_t^i$  for  $i \in E^{\text{out}}$ , and the variables  $\bar{\gamma}_t^i$  and  $\bar{h}_t^i$  for  $i \in E^{\text{in}}$  play the roles of ghost states and shall be specified below. For ease of notation, we introduce the column vectors

$$\begin{aligned}
 \boldsymbol{\rho}_t &= \left( (\rho_{t,k}^i)_{k=0}^{n_L^i} \right)_{i \in E}, & \text{for } t = 0, \dots, n_T, \\
 \hat{\boldsymbol{\gamma}}_t &= (\hat{\gamma}_t^i)_{i \in E \setminus E^{\text{out}}}, & \bar{\boldsymbol{\gamma}}_t &= (\bar{\gamma}_t^i)_{i \in E \setminus E^{\text{in}}}, & \text{for } t = 0, \dots, n_T - 1, \\
 \hat{\boldsymbol{h}}_t &= (\hat{h}_t^i)_{i \in E \setminus E^{\text{out}}}, & \bar{\boldsymbol{h}}_t &= (\bar{h}_t^i)_{i \in E \setminus E^{\text{in}}}, & \text{for } t = 0, \dots, n_T - 1.
 \end{aligned}$$

**3.1. Dynamic constraints.** For the moment, let the traffic light configuration be fixed to  $a^s$  for some  $s \in \Omega$ . The sLxF scheme can then be formulated as

$$\rho_{t+1,k}^i = \frac{\rho_{t,k-1}^i + 2\rho_{t,k}^i + \rho_{t,k+1}^i}{4} - \frac{\Delta t}{2\Delta x^i} (f_{s,i,k}^+(\rho_{t,k+1}^i, \rho_{t,k}^i, \hat{\gamma}_t^i) - f_{s,i,k}^-(\rho_{t,k}^i, \rho_{t,k-1}^i, \bar{\gamma}_t^i)), \quad (3.1)$$

for  $i \in E, t = 0, \dots, n_T - 1$ , and  $k = 0, \dots, n_L^i$ , with numerical flux functions

$$f_{s,i,k}^+(\rho_+, \rho_0, \hat{\gamma}) = \begin{cases} 2a_i^s \hat{\gamma} - f(\rho_0) & \text{for } k = n_L^i, i \in E \setminus E^{\text{out}}, \\ 2f(\rho_0) & \text{for } k = n_L^i, i \in E^{\text{out}}, \\ f(\rho_+) & \text{otherwise,} \end{cases}$$

$$f_{s,i,k}^-(\rho_0, \rho_-, \bar{\gamma}) = \begin{cases} 2\bar{\gamma} - f(\rho_0) & \text{for } k = 0, i \in E \setminus E^{\text{in}}, \\ 2f(\rho_-) & \text{for } k = n_L^i, i \in E^{\text{out}}, \\ f(\rho_-) & \text{otherwise.} \end{cases}$$

We immediately observe that really only  $f^+$  depends on  $s$  through the occurrence of  $a_i^s$  in the first case.

For  $t = 0, \dots, n_T - 1$  we now define the ghost states implicitly to incorporate the boundary conditions (2.3), (2.4), and the free outflow conditions at outgoing edges according to

$$\rho_{t,-1}^i = \begin{cases} \rho_i^{\text{in}}(t\Delta t) & \text{for } i \in E^{\text{in}}, \\ \rho_{t,0}^i & \text{for } i \in E \setminus E^{\text{in}}, \end{cases} \quad \rho_{t,n_L^i+1}^i = \begin{cases} \rho_{t,n_L^i-1}^i & \text{for } i \in E^{\text{out}}, \\ \rho_{t,n_L^i}^i & \text{for } i \in E \setminus E^{\text{out}}, \end{cases} \quad (3.2)$$

$$\bar{\gamma}_t^i = f(\rho_i^{\text{in}}(t\Delta t)) \quad \text{for } i \in E^{\text{in}}, \quad \hat{\gamma}_t^i = 0 \quad \text{for } i \in E^{\text{out}}.$$

The fluxes  $\hat{\gamma}_t, \bar{\gamma}_t, \hat{h}_t, \bar{h}_t$  are determined via the conditions (2.5c)–(2.5d) that require for  $t = 0, \dots, n_T - 1$

$$\hat{\gamma}_t^i \leq f(\min(\rho_{t,n_L^i}^i, \rho^*)) \quad \text{for } i \in E \setminus E^{\text{out}} \quad \text{and} \quad \bar{\gamma}_t^i \leq f(\max(\rho_{t,0}^i, \rho^*)) \quad \text{for } i \in E \setminus E^{\text{in}},$$

which we bring to a differentiable formulation

$$\begin{aligned} \hat{\gamma}_t^i &\leq f(\hat{h}_t^i) & \hat{h}_t^i &\leq \rho^*, & \hat{h}_t^i &\leq \rho_{t,n_L^i}^i, & \text{for } i \in E \setminus E^{\text{out}}, \\ \bar{\gamma}_t^i &\leq f(\bar{h}_t^i) & \bar{h}_t^i &\geq \rho^*, & \bar{h}_t^i &\geq \rho_{t,0}^i, & \text{for } i \in E \setminus E^{\text{in}}, \end{aligned} \quad (3.3)$$

via the slack variables

$$\hat{h}_t^i = \min(\rho_{t,n_L^i}^i, \rho^*) \quad \text{for } i \in E \setminus E^{\text{out}} \quad \text{and} \quad \bar{h}_t^i = \max(\rho_{t,0}^i, \rho^*) \quad \text{for } i \in E \setminus E^{\text{in}}.$$

The junction entropy condition (2.8) in discretized form reads

$$\max \sum_{i \in \delta_v^{\text{in}}} \bar{\gamma}_t^i \quad \text{for all } v \in V, t = 0, \dots, n_T - 1. \quad (3.4)$$

In order to describe the traffic distribution at junctions, we can now discretize (2.7) as

$$\bar{\gamma}_t^j = \sum_{i \in \delta_v^{\text{in}}} d_{ij} a_j^s \hat{\gamma}_t^i \quad \text{for all } t = 0, \dots, n_T - 1, j \in \delta_v^{\text{out}}, v \in V^{\text{io}}.$$

Finally, we assume that the initial conditions for the densities are provided in  $\rho_{0,k}^i$  for  $i \in E, k = 0, \dots, n_L^i$ . This completes the discretization of the traffic flow equations as differentiable dynamic constraints. We remark here that for numerical stability, the discretization grid must satisfy the Courant-Friedrichs-Levy (CFL) condition

$$C_{\text{CFL}} \Delta t \leq \Delta x^i \quad \text{for all } i \in E, \quad (3.5)$$

where  $C_{\text{CFL}} = 2 \|f'\|_\infty$  depends on the maximum norm of the derivative  $f' : [0, 1] \rightarrow \mathbb{R}$  of the flow function. In addition, it is necessary for the convergence of the sLxF scheme that an inverse CFL condition of the form

$$\Delta x^i \leq c \Delta t \quad \text{for some constant } c > 0 \quad (3.6)$$

is satisfied (cf. §3.2).

**3.2. Decoupling of temporal and spatial discretization.** In §4, we shall require that  $\Delta t$  can be made arbitrarily small in comparison to  $\Delta x^i, i \in E$ , so that the inverse CFL condition (3.6) cannot hold. The sLxF method achieves its simplicity by introduction of an artificial diffusion term in (2.1) according to

$$\partial_t \rho_i + \partial_x f(\rho_i) = \nu^i \partial_{xx} \rho_i \quad \text{on } [0, T] \times [0, L_i], i \in E, \quad (3.7)$$

for some small  $\nu^i > 0, i \in E$ . If we apply standard Finite Differences to the parabolic equation (3.7), we obtain

$$\begin{aligned} \rho_{t+1,k}^i &= \rho_{t,k}^i + \nu^i \Delta t \frac{\rho_{t,k-1}^i - 2\rho_{t,k}^i + \rho_{t,k+1}^i}{(\Delta x^i)^2} \\ &\quad - \frac{\Delta t}{2\Delta x^i} (f_{s,i,k}^+(\rho_{t,k+1}^i, \rho_{t,k}^i, \hat{\gamma}_t^i) - f_{s,i,k}^-(\rho_{t,k}^i, \rho_{t,k-1}^i, \bar{\gamma}_t^i)) \end{aligned} \quad (3.8)$$

for  $i \in E, t = 0, \dots, n_T - 1$ , and  $k = 0, \dots, n_L^i$ . With the choice

$$\nu^i = (\Delta x^i)^2 / (4\Delta t), \quad (3.9)$$

we recover the sLxF scheme (3.1) for the hyperbolic equation (2.1). Apparently, the coefficient  $\nu^i$  of the diffusion terms depend on the chosen discretization. The inverse CFL condition (3.6) ensures that  $\nu^i \rightarrow 0$  as  $\Delta t \rightarrow 0$ . In contrast, if  $\Delta x^i$  stays bounded away from 0 then  $\nu^i \rightarrow \infty$  as  $\Delta t \rightarrow 0$  and the traffic flow dynamics are completely overpowered by the strong diffusion term.

We stage all further analysis in the setting of (3.7) and (3.8) with fixed  $\nu^i$  (independent of  $\Delta t$  and  $\Delta x^i$ ) instead of (2.1) and (3.1), knowing that (3.1) and (3.8) coincide for the choice (3.9).

After substitution of the ghost states (3.2) in (3.8), we arrive at the vectorial short form

$$\rho_{t+1} = \rho_t + \Delta t \Phi^s(t, \rho_t, \hat{\gamma}_t, \bar{\gamma}_t, \hat{h}_t, \bar{h}_t) \quad \text{for } t = 0, \dots, n_T - 1, \quad (3.10)$$

where the function  $\Phi^s$  depends on the current traffic light configuration  $a^s$ .

**3.3. Combinatorial constraints that couple over time.** In order to obtain useful traffic light programs, we have to enforce further constraints in practice. As in [9], we consider upper time limits on red phases and lower limits on green phases. These constraints impose an additional combinatorial complexity on the traffic light optimization problem, because in their presence the control decisions are tightly coupled over whole time intervals. This property leads to detrimental effects in the application of the POC approach, see §4.

**3.4. Discretized optimization problem.** In order to provide a complete description of the discretized optimization problem in disjunctive form, we also discretize the binary function  $\omega(t)$  on the time grid, denoted by

$$\omega_t = (\omega_t^s)_{s=1}^{n_\Omega} \in \{0, 1\}^{n_\Omega} \quad \text{for } t = 0, \dots, n_T - 1.$$

We finally arrive at the large-scale mixed-integer nonlinear optimization problem

$$\begin{aligned} & \max_{\substack{\omega_t, \hat{\gamma}_t, \bar{\gamma}_t, \hat{h}_t, \bar{h}_t, \\ t=0, \dots, n_T-1, \\ \rho_t, t=1, \dots, n_T}} \sum_{i \in E} \sum_{t=1}^{n_T} \sum_{k=0}^{n_L^i} f(\rho_{t,k}^i) \Delta x^i \Delta t + \sum_{i \in E \setminus E^{\text{in}}} \sum_{t=0}^{n_T-1} \bar{\gamma}_t^i \Delta t, \\ & \text{subject to} \quad \bigvee_{s=1}^{n_\Omega} \left[ \begin{aligned} & \omega_t^s = 1 \\ & \rho_{t+1} = \rho_t + \Delta t \Phi^s(t, \rho_t, \hat{\gamma}_t, \bar{\gamma}_t, \hat{h}_t, \bar{h}_t) \\ & \bar{\gamma}_t^j = \sum_{i \in \delta_v^{\text{in}}} d_{ij} a_j^s \hat{\gamma}_t^i, \quad \forall j \in \delta_v^{\text{out}}, v \in V^{\text{io}} \end{aligned} \right] \quad \forall t = 0, \dots, n_T - 1, \\ & \hat{\gamma}_t^i \leq f(\hat{h}_t^i), \hat{h}_t^i \leq \rho^*, \hat{h}_t^i \leq \rho_{t,n_L^i}^i, \quad \forall i \in E \setminus E^{\text{out}}, t = 0, \dots, n_T - 1, \\ & \bar{\gamma}_t^i \leq f(\bar{h}_t^i), \bar{h}_t^i \geq \rho^*, \bar{h}_t^i \geq \rho_{t,0}^i, \quad \forall i \in E \setminus E^{\text{in}}, t = 0, \dots, n_T - 1, \\ & \text{and additional combinatorial constraints coupling over time.} \end{aligned} \tag{3.11}$$

We remark here that MINLP (3.11) is really a discretization of a relaxation of (2.10), for which the feasible set has been enlarged by omission of the flow distribution optimality principle (2.8). To incorporate its discretized form (3.4) in (3.11) would lead to a bilevel optimization problem (see, e.g., [6, 4]) with  $n_T$  lower level problems. Within the two-stage approach outlined in §5, the bilevel approach would yield a stronger approximation result, but at the expense of a much more challenging numerical approach for the nonlinear optimization problem of Stage I. Hence, we consider the MINLP formulation (3.11) in the remainder of this article.

**4. Partial Outer Convexification.** The disjunctive formulation of problem (3.11) can be transformed to a conventional MINLP formulation by the use of convex combinations, where the entries of  $\omega_t$  serve as convex multipliers. If the integrality condition on  $\omega_t$  is kept, problem (3.11) can be equivalently cast as

$$\begin{aligned} & \max_{\substack{\omega_t, \hat{\gamma}_t, \bar{\gamma}_t, \hat{h}_t, \bar{h}_t, \\ t=0, \dots, n_T-1, \\ \rho_t, t=1, \dots, n_T}} \sum_{i \in E} \sum_{t=1}^{n_T} \sum_{k=0}^{n_L^i} f(\rho_{t,k}^i) \Delta x^i \Delta t + \sum_{i \in E \setminus E^{\text{in}}} \sum_{t=0}^{n_T-1} \bar{\gamma}_t^i \Delta t, \\ & \text{subject to} \quad \left. \begin{aligned} & \sum_{s=1}^{n_\Omega} \omega_t^s = 1 \\ & \rho_{t+1} = \rho_t + \Delta t \Phi(t, \rho_t, \hat{\gamma}_t, \bar{\gamma}_t, \hat{h}_t, \bar{h}_t) \omega_t \\ & \bar{\gamma}_t^j = \sum_{s=1}^{n_\Omega} \sum_{i \in \delta_v^{\text{in}}} d_{ij} a_j^s \hat{\gamma}_t^i \omega_t^s, \quad \forall j \in \delta_v^{\text{out}}, v \in V^{\text{io}} \\ & \hat{\gamma}_t^i \leq f(\hat{h}_t^i), \hat{h}_t^i \leq \rho^*, \hat{h}_t^i \leq \rho_{t,n_L^i}^i, \quad \forall i \in E \setminus E^{\text{out}} \\ & \bar{\gamma}_t^i \leq f(\bar{h}_t^i), \bar{h}_t^i \geq \rho^*, \bar{h}_t^i \geq \rho_{t,0}^i, \quad \forall i \in E \setminus E^{\text{in}} \end{aligned} \right\} \quad \forall t = 0, \dots, n_T - 1, \\ & \text{and additional combinatorial constraints coupling over time,} \end{aligned} \tag{4.1}$$

where the  $s$ -th column of the matrix-valued function  $\Phi$  is constituted by the function  $\Phi^s$  for  $s = 1, \dots, n_\Omega$  from (3.10).



**5. Computation of near-optimal solutions.** The aim of this article is to devise a fast heuristic for approximate solutions of (2.9) via the generation of feasible points of (4.1) with near-optimal objective value. We follow the approach in [21, 13, 14, 15] and split up the solution of the MINLP (4.1) into two stages. Stage one comprises the solution of one NLP and stage two the solution of one MILP without dynamic constraints in which the solution of stage one enters as data.

Our computational approach can be outlined in the following steps:

1. **Discretize** by choosing suitable spatial mesh sizes  $\Delta x^i > 0, i \in E$ . Relax problem by omitting (3.4).
2. **Smooth** the dynamics by determining the maximal CFL-compatible sLxF time step  $\Delta t_{\text{CFL}}$  to define the artificial diffusion coefficients

$$\nu^i = \frac{(\Delta x^i)^2}{4\Delta t_{\text{CFL}}} = \frac{(\Delta x^i)^2}{4 \min_{j \in E} \frac{\Delta x^j}{2\|f'\|_\infty}} = \frac{\|f'\|_\infty (\Delta x^i)^2}{2 \min_{j \in E} \Delta x^j}, \quad i \in E.$$

Initialize  $\Delta t = \Delta t_{\text{CFL}}$ .

3. Stage I: **Relax** the integrality condition

$$\omega_t \in \{0, 1\}^{n_\Omega} \rightsquigarrow \omega_t \in [0, 1]^{n_\Omega}$$

for  $t = 0, \dots, n_T - 1$  in the partially outer convexified problem (4.1) and solve the resulting continuous NLP to obtain an optimal vector  $(\omega_t^{\text{rlx}})_{t=0}^{n_T-1}$ .

4. Stage II: **Reconstruct** a binary feasible vector  $(\omega_t^{\text{bin}})_{t=0}^{n_T-1}$  as the solution of the Combinatorial Integral Approximation Problem (CIAP), an MILP without dynamic constraints in which  $(\omega_t^{\text{rlx}})_{t=0}^{n_T-1}$  enters as data.
5. **Simulate** the traffic dynamics again with  $(\omega_t^{\text{bin}})_{t=0}^{n_T-1}$  to obtain a feasible trajectory and a corresponding objective value.

Optionally, a refinement step of the temporal mesh size  $\Delta t$  can be performed after Step 4 to improve the accuracy of the switching if necessary, but this step is only useful in the case without additional combinatorial constraints that couple over time [20, 21]. We do not consider this option further in this article.

We first discuss the case in which no additional combinatorial constraints that couple over time, e.g., bounds on the minimal and maximal red and green phases of each traffic light, are present. In this case, we can give a rigorous bound on the quality of the heuristic.

**5.1. Case I: No combinatorial constraints that couple over time.** The idea for the construction of the NLP is simply the relaxation of the integrality condition  $\omega_t \in \{0, 1\}^{n_\Omega}$  to  $\omega_t \in [0, 1]^{n_\Omega}$  for  $t = 0, \dots, n_T - 1$ . The following approximation lemma is the reason why we study the optimization problem in the form (4.1) and not in a form which contains direct discretizations of the binary traffic light control  $A(t)$  like in (2.9), for which no equally strong relaxation results are known to the authors.

The lemma is a discrete version of [20, Theorem 2]. Another discrete version exists [12] and we point out the differences below. In order to state the lemma, we need the convex hull of the columns of the identity matrix

$$\mathcal{H} = \left\{ \alpha \in \mathbb{R}_{\geq 0}^{n_\Omega} \mid \sum_{i=1}^{n_\Omega} \alpha_i = 1 \right\}$$

and two norms  $\|\cdot\|_X : \mathbb{R}^n \rightarrow \mathbb{R}_{\geq 0}$  and  $\|\cdot\|_\Omega : \mathbb{R}^{n_\Omega} \rightarrow \mathbb{R}_{\geq 0}$ .

**LEMMA 5.1.** *Let  $I = \{0, \dots, n_T - 1\}$ ,  $D \subseteq \mathbb{R}^n$ , and  $\Phi : I \times D \rightarrow \mathbb{R}^{n \times n_\Omega}$  be a matrix-valued function that is continuous with respect to the second argument and*

satisfies

$$\|\Phi(t, y)v\|_X \leq M \|v\|_\Omega \quad \text{for all } t \in I, y \in D, v \in \mathbb{R}^{n_\Omega}, \quad (5.1)$$

$$\|[\Phi(t, y) - \Phi(t, \eta)]\alpha\|_X \leq L \|y - \eta\|_X \quad \text{for all } t \in I, y, \eta \in D, \alpha \in \mathcal{H} \quad (5.2)$$

for constants  $M, L < \infty$ . Furthermore, for each  $t \in I$  let  $h_t > 0, \alpha^t, \beta^t \in \mathcal{H}$  such that  $T = \sum_{t=0}^{n_T-1} h_t$  and for each  $t \in I \cup \{n_T\}$  let  $y^t, \eta^t \in D$  be given such that for all  $t \in I$

$$y^{t+1} = y^t + h_t \Phi(t, y^t) \alpha^t \quad \text{and} \quad \eta^{t+1} = \eta^t + h_t \Phi(t, \eta^t) \beta^t.$$

If for some set  $I' \subseteq I$ , constants  $C, \varepsilon < \infty$ , and some vector  $\delta^0 \in \mathbb{R}^{n_\Omega}$  it holds that

$$\|[\Phi(t+1, y^{t+1}) - \Phi(t, y^t)]v\|_X \leq h_t C \|v\|_\Omega \quad \text{for all } t \in I', v \in \mathbb{R}^{n_\Omega}, \quad (5.3)$$

$$\left\| \delta^0 + \sum_{t=0}^{k-1} h_t (\alpha^t - \beta^t) \right\|_\Omega \leq \varepsilon \quad \text{for all } k \in I \cup \{n_T\}, \quad (5.4)$$

then it follows with  $T'_k = k \max\{h_t \mid t = 0, \dots, k-1\}$  and  $n_{\text{jump}} = |I \setminus (I' \cup \{n_T - 1\})|$  that for all  $k \in I \cup \{n_T\}$

$$\sum_{t=0}^k h_t \|y^t - \eta^t\|_X \leq \frac{\exp(T'_k L) - 1}{L} (\|y^0 - \eta^0\|_X + (2M(1 + n_{\text{jump}}) + TC)\varepsilon).$$

*Proof.* For  $k \in I \cup \{n_T\}$ , we define

$$e^k = y^k - \eta^k \quad \text{and} \quad \delta^k = \delta^0 + \sum_{t=0}^{k-1} h_t (\alpha^t - \beta^t).$$

We immediately obtain

$$\begin{aligned} \|e^k\|_X &= \left\| y^0 + \sum_{t=0}^{k-1} h_t \Phi(t, y^t) \alpha^t - \eta^0 - \sum_{t=0}^{k-1} h_t \Phi(t, \eta^t) \beta^t \right\|_X \\ &= \left\| (y^0 - \eta^0) + \sum_{t=0}^{k-1} h_t \Phi(t, y^t) (\alpha^t - \beta^t) + \sum_{t=0}^{k-1} h_t (\Phi(t, y^t) - \Phi(t, \eta^t)) \beta^t \right\|_X \\ &\leq \|e^0\|_X + \left\| \sum_{t=0}^{k-1} \Phi(t, y^t) h_t (\alpha^t - \beta^t) \right\|_X + \left\| \sum_{t=0}^{k-1} h_t (\Phi(t, y^t) - \Phi(t, \eta^t)) \beta^t \right\|_X. \end{aligned} \quad (5.5)$$

We use Abel summation (the discrete version of integration by parts) and assumptions (5.1), (5.3), and (5.4) to bound the penultimate term in (5.5) according to

$$\begin{aligned} \left\| \sum_{t=0}^{k-1} \Phi(t, y^t) h_t (\alpha^t - \beta^t) \right\|_X &= \left\| \sum_{t=0}^{k-1} \Phi(t, y^t) (\delta^{t+1} - \delta^t) \right\|_X \\ &= \left\| \Phi(k-1, y^{k-1}) \delta^k - \Phi(0, y^0) \delta^0 - \sum_{t=0}^{k-2} [\Phi(t+1, y^{t+1}) - \Phi(t, y^t)] \delta^{t+1} \right\|_X \\ &\leq \|\Phi(k-1, y^{k-1}) \delta^k\|_X + \|\Phi(0, y^0) \delta^0\|_X + \sum_{t=0}^{k-2} \|\Phi(t+1, y^{t+1}) - \Phi(t, y^t)\|_X \delta^{t+1} \end{aligned}$$

$$\leq (2M + TC + 2Mn_{\text{jump}})\varepsilon,$$

where we have split up the last occurring sum over indices in  $I'$  (sum  $\leq TC\varepsilon$ ) and not in  $I'$  (sum  $\leq 2Mn_{\text{jump}}\varepsilon$ ). Using (5.2), the third term in (5.5) can be bounded as

$$\left\| \sum_{t=0}^{k-1} h_t [\Phi(t, y^t) - \Phi(t, \eta^t)] \beta^t \right\|_X \leq L \sum_{t=0}^{k-1} h_t \|e^t\|_X.$$

We finally obtain

$$\|e^k\|_X \leq \|e^0\|_X + (2M(1 + n_{\text{jump}}) + TC)\varepsilon + L \sum_{t=0}^{k-1} h_t \|e^t\|_X,$$

which is equivalent to

$$\frac{B^{k+1} - B^k}{h_k} \leq \|e^0\|_X + (2M(1 + n_{\text{jump}}) + TC)\varepsilon + LB^k, \quad \text{where } B^k = \sum_{t=0}^{k-1} h_t \|e^t\|_X,$$

which implies with  $h_k^{\max} = \max\{h_t \mid t = 0, \dots, k\}$  for all  $i \leq k$  that

$$B^{i+1} \leq h_k^{\max} \|e^0\|_X + h_k^{\max} (2M(1 + n_{\text{jump}}) + TC)\varepsilon + (1 + h_k^{\max} L)B^i.$$

A discrete version of Gronwall's inequality (see, e.g., [23]) can be used to deduce

$$B^k \leq \frac{\exp(Lkh_k^{\max}) - 1}{L} (\|e^0\|_X + (2M(1 + n_{\text{jump}}) + TC)\varepsilon).$$

The assertion

$$\sum_{t=0}^k h_t \|e^t\|_X \leq \frac{\exp(T'_k L) - 1}{L} (\|e^0\|_X + (2M(1 + n_{\text{jump}}) + TC)\varepsilon)$$

follows immediately.  $\square$

The main differences to [12] are the following:

1. The explicit use of time steps  $h_t$  ensure temporal grid-independence of the result provided that the ratio of the largest to the smallest step size (and thus  $T'_k$ ) stays bounded. (We shall observe below that the constants, however, depend on the spatial grid.)
2. We explicitly take into account “jump discontinuities” in  $I'$  due to jumps in the non-autonomous part of  $\Phi$ .
3. The initial offset  $\delta^0$  in (5.4), which is not present in [12], can be exploited in case we do not drive  $\varepsilon$  to zero.
4. We rephrased the assumptions so that no special choice for the norm  $\|\cdot\|_\Omega$  is required in the proof.

We now apply Lemma 5.1 to the following objects: We assume that we have obtained a relaxed solution  $\omega_t = \omega_t^{\text{rlx}} \in \mathcal{H}, t = 0, \dots, n_T$ , of the stage one NLP relaxation of (4.1). We then set  $n = \sum_{i \in E} (n_L^i + 1), D = [0, 1]^n$  and identify for  $t = 0, \dots, n_T - 1$

$$\begin{aligned} h_t &= \Delta t, & \Psi(t) &= \Psi(t), & \Phi(t, y) &= \Phi(t, y, \hat{\gamma}_t, \bar{\gamma}_t, \hat{h}_t, \bar{h}_t), \\ \alpha^t &= \omega_t, & y^t &= \rho_t, & y^{n_T} &= \rho_{n_T}. \end{aligned}$$

In order to verify the remaining assumptions, we choose the maximum norm on  $\mathbb{R}^{n_\Omega}$  for  $\|\cdot\|_\Omega$  and the discrete  $L^1$ -norm for densities  $\rho_t \in \mathbb{R}^n$  according to

$$\|\rho_t\|_X = \sum_{i \in E} \sum_{k=0}^{n_L^i} |\rho_{k,t}^i| \Delta x^i.$$

We now determine an integer vector  $\beta^t \in \mathcal{H} \cap \{0, 1\}^{n_\Omega}$  as the solution of the stage two MILP without dynamic constraints, called the Combinatorial Integral Approximation Problem (CIAP) [21],

$$\begin{aligned} & \min_{\substack{\beta^t \in \mathcal{H} \cap \{0, 1\}^{n_\Omega}, \\ t=0, \dots, n_T-1 \\ \delta^0 \in \mathbb{R}^{n_\Omega}, \varepsilon \in \mathbb{R}}} \varepsilon \\ \text{subject to} \quad & \left\| \delta^0 + \sum_{t=0}^{k-1} \Delta t (\omega_t - \beta^t) \right\|_\Omega \leq \varepsilon, \quad \text{for all } k = 0, \dots, n_T. \end{aligned} \quad (5.6)$$

Here we exploit that the upper bound on the norm  $\|\cdot\|_\Omega$  can be reformulated as a set of linear constraints. The objective is to minimize  $\varepsilon$  and thus the left-hand side of assumption (5.4). The corresponding densities  $\eta^t$  can then be computed based on the iteration

$$\eta^0 = y^0, \quad \eta^{t+1} = \eta^t + \Delta t \Phi(t, \eta^t) \beta^t \quad \text{for } t = 0, \dots, n_T - 1.$$

In order to show the bound (5.1), we arbitrarily choose  $t \in I \cup \{n_T\}$ ,  $y = \rho_t \in D$ , and  $v \in \mathbb{R}^{n_\Omega}$  and observe that with  $\Delta x_{\min} := \min_{i \in E} \Delta x^i$  and  $\nu_{\max} = \max_{i \in E} \nu^i$

$$\begin{aligned} \|\Phi(t, \rho_t) v\|_X &= \sum_{i \in E} \sum_{k=0}^{n_L^i} \left| \sum_{s=1}^{n_\Omega} \left( \nu^i \frac{\rho_{t,k-1}^i - 2\rho_{t,k}^i + \rho_{t,k+1}^i}{(\Delta x^i)^2} \right. \right. \\ &\quad \left. \left. + \frac{f_{s,i,k}^+(\rho_{t,k+1}^i, \rho_{t,k}^i, \hat{\gamma}_t^i) - f_{s,i,k}^-(\rho_{t,k}^i, \rho_{t,k-1}^i, \bar{\gamma}_t^i)}{2\Delta x^i} \right) v_s \right| \Delta x^i \\ &\leq \sum_{i \in E} \sum_{k=0}^{n_L^i} \left( \frac{4\nu^i}{(\Delta x^i)^2} + \frac{2f(\rho^*)}{2\Delta x^i} \right) \sum_{s=1}^{n_\Omega} |v_s| \Delta x^i \\ &\leq \frac{4\nu_{\max} + f(\rho^*)\Delta x_{\min}}{\Delta x_{\min}^2} n_\Omega \left( \sum_{i \in E} L^i \right) \|v\|_\Omega =: M \|v\|_\Omega. \end{aligned}$$

We now investigate the Lipschitz assumption (5.2). To this end, we additionally choose  $\eta = \eta_t \in D$  and  $\alpha \in \mathcal{H}$ . Let  $L_f \geq 1$  denote the Lipschitz constant of the flow function  $f$ . We then obtain

$$\begin{aligned} \left| f_{s,i,k}^+(\rho_+, \rho_\circ, \hat{\gamma}) - f_{s,i,k}^+(\eta_+, \eta_\circ, \hat{\gamma}') \right| &\leq 2L_f (|\rho_+ - \eta_+| + |\rho_\circ - \eta_\circ| + |\hat{\gamma} - \hat{\gamma}'|), \\ \left| f_{s,i,k}^-(\rho_\circ, \rho_-, \bar{\gamma}) - f_{s,i,k}^-(\eta_\circ, \eta_-, \bar{\gamma}') \right| &\leq 2L_f (|\rho_\circ - \eta_\circ| + |\rho_- - \eta_-| + |\bar{\gamma} - \bar{\gamma}'|). \end{aligned} \quad (5.7)$$

Hence, we can deduce that

$$\|[\Phi(t, \rho_t) - \Phi(t, \eta_t)] \alpha\|_X$$

$$\begin{aligned}
&= \sum_{i \in E} \sum_{k=0}^{n_L^i} \left| \sum_{s=1}^{n_\Omega} \left( \nu^i \frac{\rho_{t,k-1}^i - 2\rho_{t,k}^i + \rho_{t,k+1}^i - \eta_{t,k-1}^i + 2\eta_{t,k}^i - \eta_{t,k+1}^i}{(\Delta x^i)^2} \right. \right. \\
&\quad \left. \left. + \frac{1}{2\Delta x^i} \left( f_{s,i,k}^+(\rho_{t,k+1}^i, \rho_{t,k}^i, \hat{\gamma}_t^i) - f_{s,i,k}^-(\rho_{t,k}^i, \rho_{t,k-1}^i, \bar{\gamma}_t^i) \right. \right. \right. \\
&\quad \left. \left. \left. - f_{s,i,k}^+(\eta_{t,k+1}^i, \eta_{t,k}^i, \hat{\gamma}_t^i) + f_{s,i,k}^-(\eta_{t,k}^i, \eta_{t,k-1}^i, \bar{\gamma}_t^i) \right) \right) \alpha_s \right| \Delta x^i \\
&\leq \frac{4\nu_{\max} + 2L_f \Delta x_{\min}}{\Delta x_{\min}^2} n_\Omega \|\rho_t - \eta_t\|_X =: L \|\rho_t - \eta_t\|_X.
\end{aligned}$$

We use (5.7) again to finally address assumption (5.3). It turns out that we must require the additional assumption that there exist constants  $C_\gamma \in \mathbb{R}$  and  $n_{\text{jump}} \in \mathbb{N}$  such that for all  $\Delta t > 0$  and  $i \in E$

$$|\hat{\gamma}_{t+1}^i - \hat{\gamma}_t^i| + |\bar{\gamma}_{t+1}^i - \bar{\gamma}_t^i| \leq \Delta t C_\gamma \quad \text{for all } t \in I \text{ except for } n_{\text{jump}} \text{ exceptions.} \quad (5.8)$$

We can then deduce that

$$\begin{aligned}
&\| [\Phi(t+1, \rho_{t+1}) - \Phi(t, \rho_t)] v \|_X \\
&= \sum_{i \in E} \sum_{k=0}^{n_L^i} \left| \sum_{s=1}^{n_\Omega} \left( \nu^i \frac{\rho_{t+1,k-1}^i - 2\rho_{t+1,k}^i + \rho_{t+1,k+1}^i - \rho_{t,k-1}^i + 2\rho_{t,k}^i - \rho_{t,k+1}^i}{(\Delta x^i)^2} \right. \right. \\
&\quad \left. \left. + \frac{1}{2\Delta x^i} \left( f_{s,i,k}^+(\rho_{t+1,k+1}^i, \rho_{t+1,k}^i, \hat{\gamma}_{t+1}^i) - f_{s,i,k}^-(\rho_{t+1,k}^i, \rho_{t+1,k-1}^i, \bar{\gamma}_{t+1}^i) \right. \right. \right. \\
&\quad \left. \left. \left. - f_{s,i,k}^+(\rho_{t,k+1}^i, \rho_{t,k}^i, \hat{\gamma}_t^i) + f_{s,i,k}^-(\rho_{t,k}^i, \rho_{t,k-1}^i, \bar{\gamma}_t^i) \right) \right) v_s \right| \Delta x^i \\
&\leq \sum_{i \in E} \sum_{k=0}^{n_L^i} \left| \sum_{s=1}^{n_\Omega} \left( \frac{\nu^i \Delta t}{(\Delta x^i)^2} (\Phi_{k-1}^s(t, \rho_t) - 2\Phi_k^s(t, \rho_t) + \Phi_{k+1}^s(t, \rho_t)) \right. \right. \\
&\quad \left. \left. + \frac{2L_f \Delta t}{2\Delta x^i} (|\Phi_{k+1}^s(t, \rho_t)| + 2|\Phi_k^s(t, \rho_t)| + |\Phi_{k-1}^s(t, \rho_t)|) \right. \right. \\
&\quad \left. \left. + \frac{2L_f}{2\Delta x^i} (|\hat{\gamma}_{t+1}^i - \hat{\gamma}_t^i| + |\bar{\gamma}_{t+1}^i - \bar{\gamma}_t^i|) \right) v_s \right| \Delta x^i \\
&\leq \Delta t \left( \frac{4\nu_{\max} M + 4L_f M \Delta x_{\min}}{(\Delta x_{\min})^2} + \frac{L_f C_\gamma n_\Omega}{\Delta x_{\min}} \right) \|v\|_\Omega \\
&=: \Delta t C \|v\|_\Omega
\end{aligned}$$

for all  $t \in I$  except for  $n_{\text{jump}}$  exceptions.

For each spatial discretization we thus obtain the required constants  $M, L < \infty$ , which grow with  $\mathcal{O}(1/\min_{i \in E} \Delta x^i)$ , however, and are thus not fully grid independent.

**5.2. Case II: Additional combinatorial constraints that couple over time.** In the presence of upper and lower time limits  $T_{\text{red}}$  and  $T_{\text{green}}$  on red and green phases, we still perform Steps 1–3 and 5. Only the reconstruction in Step 4 changes slightly because we add the additional combinatorial constraints to CIAP (5.6) in Stage II (cf. [21]). They read

$$\begin{aligned}
&k + \left\lfloor \frac{T_{\text{red}}}{\Delta t} \right\rfloor + 1 \\
&\sum_{t=k+1} \sum_{s \in \Omega} a^s \beta_s^t \geq 1, \quad \text{for } k = 0, \dots, n_T - \left\lfloor \frac{T_{\text{red}}}{\Delta t} \right\rfloor - 2,
\end{aligned}$$

$$k + \left\lfloor \frac{T_{\text{green}}}{\Delta t} \right\rfloor \sum_{t=k+1}^{\left\lfloor \frac{T_{\text{green}}}{\Delta t} \right\rfloor} \sum_{s \in \Omega} a^s \beta_s^t \geq \sum_{s \in \Omega} a^s \left\lfloor \frac{T_{\text{green}}}{\Delta t} \right\rfloor (\beta_s^{k+1} - \beta_s^k), \quad \text{for } k = 0, \dots, n_T - \left\lfloor \frac{T_{\text{green}}}{\Delta t} \right\rfloor - 1.$$

Because these constraints are linear, the CIAP is still an MILP and can be solved with standard solvers. However, they render the Stage II CIAP MILP much harder than in case I without additional combinatorial constraints: While it can be shown [21] that CIAP (5.6) in Case I allows for a polynomial-time solution with optimal value  $\varepsilon \leq \Delta t/2$ , the Stage II CIAP MILP in the presence of additional combinatorial constraints is much harder to solve and no a-priori objective upper bounds on  $\varepsilon$  in terms of  $\Delta t$  can be given. The approximation Lemma 5.1 can still be invoked, but  $\varepsilon$  cannot be driven to zero by reducing  $\Delta t$  anymore. Thus, the integer optimality gap cannot be driven to zero, either. In practice, however, the two-stage approach still produces useful answers for practical purposes, see §6.

**5.3. A note on degeneracy.** From a practical optimization point of view, also the Stage I NLP in relaxed POC form can be difficult to solve due to degenerate solutions. For instance, it is quite likely that in the optimal solution some of the traffic density values  $\rho_{t,k}^i$  at the edge boundaries  $k \in \{0, n_L^i\}$  attain the value  $\rho^*$  of maximum flow. In this case, several constraints of (3.3) are active and linearly dependent. Hence, the Linear Independence Constraint Qualification (LICQ) is not satisfied in the solution. However, LICQ is often needed to guarantee convergence of NLP solvers. For primal-dual interior point methods (see, e.g., [24]), which are based on following a central path parameterized by some scalar  $\mu \geq 0$ , the existence of the central path at the solution  $\mu = 0$  cannot be guaranteed by the Implicit Function Theorem if LICQ is violated. One needs to rely on implementation specific heuristics in this case, which are luckily often highly efficient.

**6. Numerical results.** In this section we analyse the benefits of the POC approach for the nonlinear traffic light optimization problem in various aspects: We compare the efficiency of the two-stage heuristic (described in §4) with other heuristical approaches for different road networks with various grid sizes and amounts of combinatorial dependencies (i.e. we optionally include bounds on switching times as described in Section 3.3. Furthermore, we consider the optimization of the full nonlinear problem and discuss the benefits of POC-formulations and heuristic initial solution guesses for warm-starts.

All computations are performed on a PC equipped with 8 GB RAM and an Intel(R) Core(TM) i5-3470 CPU 3.20GHz. Continuous nonlinear optimization problems are solved with the open source interior-point optimizer Ipopt, version 3.12, [24]. For linear mixed integer optimization we use either CPLEX, version 12.5, [5] or SCIP, version 3.2.0, [22, 1, 25, 17]. For solving nonlinear mixed integer problems, we use Ipopt within SCIP.

**6.1. Parameter settings and scenarios.** In this article, we restrict ourselves to the quadratic flow function

$$f(\rho) = \frac{v^{\max}}{\rho^{\max}} \cdot \rho \cdot (\rho^{\max} - \rho) \quad (6.1)$$

with  $\rho^{\max} = 1$  and  $v^{\max} = 1$ . Obviously,  $f$  satisfies  $f(0) = f(1) = 0$  and has a unique strict maximum  $f(\rho^*) = \frac{1}{4}$  at  $\rho^* = \frac{1}{2}$ . In accordance with the CFL condition (3.5) we choose  $\Delta t = \frac{1}{2} \Delta x^i$ .

In the sequel, we examine the following scenarios:

**2x2-junction.** We consider a 2x2-junction as shown in Figure 6.1.

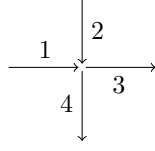
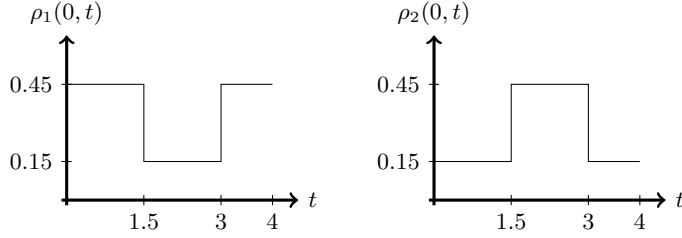


Figure 6.1: Network of a 2x2junction.

All roads have the length  $L_i = 1$ . The initial traffic density is set to  $\rho_0 = 0.1$  and the incoming boundary density is given as shown in Figure 6.2. The traffic distribution is 50% to road 3 and 50% to road 4 from each of the incoming roads, i.e.  $d_{1,3} = d_{1,4} = d_{2,3} = d_{2,4} = 0.5$ .



(a) Left boundary density of road 1. (b) Left boundary density of road 2.

Figure 6.2: Boundary density of incoming roads 1 and 2.

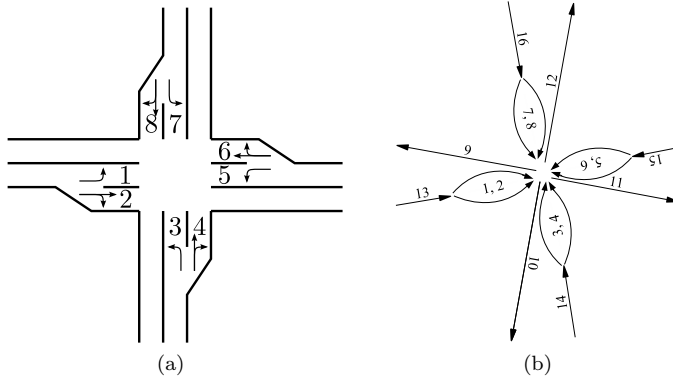


Figure 6.3: A traffic junction with eight traffic lights. Each lane is modeled by a separate edge.

**8x4-junction.** Furthermore, we consider a junction with eight traffic lights as presented in [9], see Figure 6.3. Each of the four incoming roads split into two lanes

(left turn lane and straight/right turn lane) in front of the junction. Together with the four outgoing roads, the complete network consists of 16 edges (roads).

The incoming boundary flow, road lengths  $L_i$  are set like in [9, p16]. The distribution of traffic at branching points is for all four direction the following: 10% of the traffic goes to the left turning lane and 90% to the straight/right turning lane, from which again 70% go straight and 30% turn to the right.

For both scenarios, we consider a coarse discretization grid with grid sizes  $\Delta t = 0.1$  and  $\Delta x = 0.2$  as well as a finer discretization with  $\Delta t = 0.05$  and  $\Delta x = 0.1$ . The time horizon is set to  $T = 4$ .

**6.2. Two-stage heuristic with POC approach.** We consider the heuristical strategy as described in Section 5.

The relaxed NLP obtained by partial outer convexification (see 4) yields a relaxed solution of the original traffic light optimization problem (2.9). In Stage I, we solve it with Ipopt.

In Stage II we use the  $\omega$ -values of the obtained solution as input for CIAP which is then solved by a linear mixed-integer optimization solver. Here we use SCIP as well as CPLEX and compare the results. At this point we can optionally include the additional upper and lower bounds on red and green phases of traffic lights in CIAP.

As a last step we use the optimal traffic light setting obtained in Stage II and compute the forward solution (including the intersection flux maximization (3.4) left out in (3.11)) yielding the corresponding values for traffic density and flow of the original nonlinear traffic light optimization problem (2.9).

The optimal solution  $\omega$  obtained in Stage I and the resulting optimal traffic light setting obtained after Stage II (on the one hand by the solver SCIP and on the other hand by the solver CPLEX) are shown in Figure 6.4 for the 2x2-junction for different grid sizes.

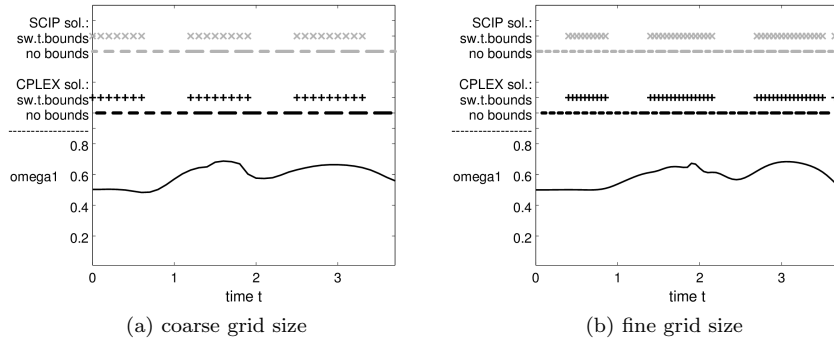


Figure 6.4: Results for road 1 in 2x2-junction. The first four lines show the time of the green phases of traffic light 1 using solver SCIP and CPLEX and regarding additional conditions on upper and lower bound on switching times as described in Section 3.3 and the curve below shows  $\omega_1$ .

For the 2x2-junction scenarios,  $\Omega$  has two elements.  $\omega_1 = 1$  corresponds to the situation where traffic light 1 is green and traffic light 2 is red and vice versa for  $\omega_2$ .

The results for all considered scenarios are shown in Table 6.1.



Stage I				Stage II			
vars	OFV (IpOpt)	time of POC	swt bnds	vars of CIAP	solver	OFV of fwd sol	time
2x2-junction coarse grid ( $\Delta t = 0.1$ )							
1704	3.6451	0.93s	no	161	SCIP	3.6467	2.16s
					CPLEX	3.6582	0.19s
			yes	83	SCIP	3.6118	0.32s
					CPLEX	3.6118	0.12s
2x2-junction fine grid ( $\Delta t = 0.05$ )							
5004	3.3948	5.70s	no	321	SCIP	3.4020	32.93s
					CPLEX	3.3851	2.31s
			yes	163	SCIP	3.3375	2.18s
					CPLEX	3.3373	0.68s
8x4-junction coarse grid ( $\Delta t = 0.1$ )							
7300	20.7062	91.35s	no	1281	SCIP	20.7657	12.82s
					CPLEX	20.7099	1.41s
			yes	657	SCIP	20.3205	>1h*
					CPLEX	20.2632	>1h*
8x4-junction fine grid ( $\Delta t = 0.05$ )							
20656	18.7653	675.78s	no	2561	SCIP	18.7817	423.42s
					CPLEX	18.7642	19.62s
			yes	1297	SCIP	18.0658	>1h*
					CPLEX	18.1359	>1h*

Table 6.1: Two-stage heuristic.

Table 6.1 does not show the objective function value of the optimal solution of CIAP, but the objective function value, that the resulting traffic light setting would yield in the original problem (2.9). The “\*” means that the solution process has been interrupted (after one hour). Hence, the resulting solution is not necessarily globally optimal for CIAP.

The optimal solution of CIAP is not unique. Depending on the parameter setting of the solvers, different solution can be found. Different optimal solution of CIAP do not necessarily yield the same objective function value in the original problem. (That is why the OFV obtained by SCIP and CPLEX differ most of the time from each other.) CPLEX solves the CIAP faster than SCIP in all cases, however, the solution found by SCIP leads in most of the cases to a better primal bound of the original problem.

We can also observe, that for both solvers, it is much harder to solve a problem which is highly combinatorially interconnected problem, even though it might have considerably less variables than another one. For example, the CIAP for the 8x4-junction with additional restrictions on switching times is even for the coarse grid ( $\rightarrow$  657 variables) much harder to solve, than the 8x4junction without those restrictions for the fine grid ( $\rightarrow$  2561 variables).

**6.3. MILP heuristic.** Another possibility to obtain heuristic solutions, is to linearize the problem (2.9). When we use a piecewise linear flow function as in [9], namely

$$\tilde{f} = \begin{cases} \lambda \cdot \rho & \text{if } 0 \leq \rho \leq \rho^* \\ \lambda \cdot (2\rho^* - \rho) & \text{if } \rho^* < \rho \leq \rho^{\max} \end{cases} \quad (6.2)$$

with  $\lambda = 0.5$ ,  $\rho^* = 0.5$  and  $\rho^{\max} = 1$ , cf. Figure 6.5, then we can apply various linearization techniques and solve the resulting linear MIP for example by CPLEX, as done in [9].

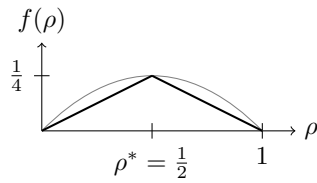


Figure 6.5: Piecewise linear vs. quadratic flow function.

However, the dynamical behavior of the traffic using each of these flow functions differ considerably from each other. A traffic density evolution of the 2x2-junction with even traffic light switching periods for both flow functions is shown in Figure 6.6. Hence, the optimal solution of the linearized version is not necessarily close to the optimal solution of the nonlinear model. However, we can use the resulting traffic light setting as heuristic solution.

Now, we compute optimal solutions of the linear MIP by CPLEX. Then, a forward simulation using the nonlinear flow function computes the corresponding objective function value for the original flow problem.

The results are shown in Table 6.2.

Scenario	# vars	swt bnds	OFV (fwd sol)	time	gap
2x2 (coarse)	5740	no	3.4640	320.67s	0%
		yes	3.5039	3.98s	0%
2x2 (fine)	17820	no	3.2042	>1h	1.31%
		yes	3.2730	236.31s	0%
8x4 (coarse)	23616	no	20.7709	>1h	0.08%
		yes	out of memory		
8x4 (fine)	71280	no	18.6484	>1h	0.71%
		yes	out of memory		

Table 6.2: MILP heuristic.

The MILP heuristic does not yield as good primal bounds as the two-stage heuristic. The only exception, where the MILP approach is better, is for the 8x4-junction with coarse discretization grid without restrictions on the switching times.

In Fig. 6.7–6.8, the traffic light settings given by the two-stage heuristic (using CPLEX) and the MILP heuristic are shown. In Fig. 6.7, no restrictions on the traffic

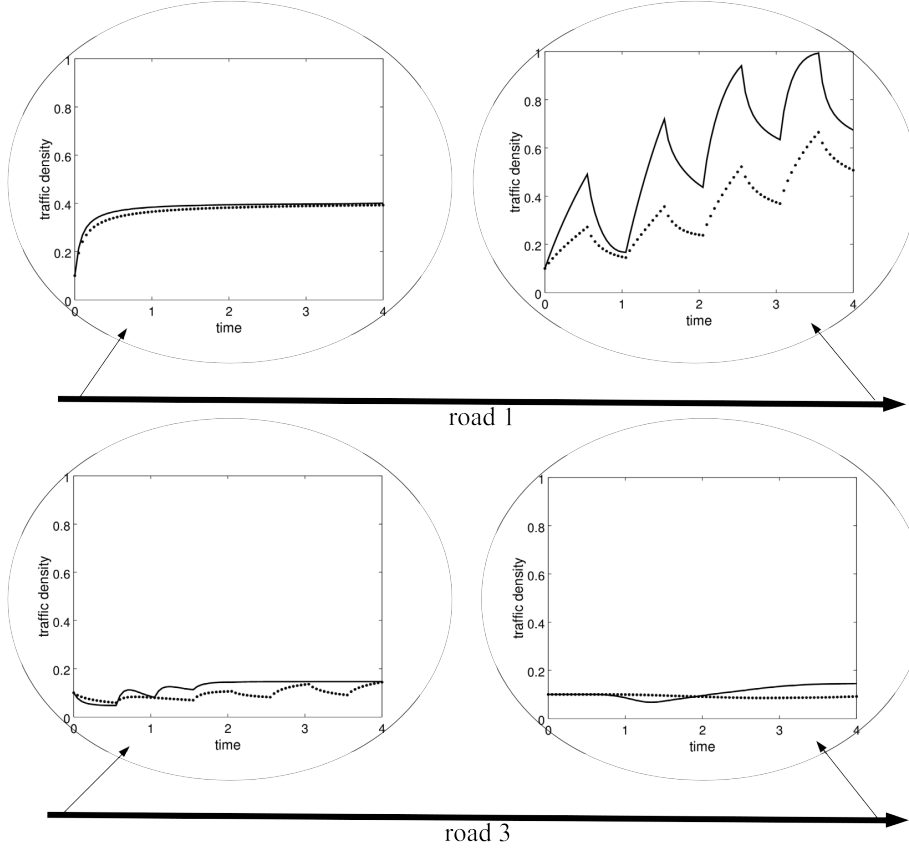


Figure 6.6: Comparison of traffic density evolution for different points of the traffic network. The black lines denote the traffic density using the smooth flow function (6.1) and the dotted lines denote the traffic density using the piecewise linear flow function (6.2).

lights are given. Here we can see, that the left-turning lanes are kept red during the whole time horizon, since only a small part of the traffic is using it. If we add upper bounds for red phases (and lower bounds for green phases), this effect is avoided, see Fig. 6.8.

**6.4. Optimizing nonlinear MIP with SCIP.** Now, we want to solve the complete nonlinear mixed-integer problem directly. SCIP is a solver that uses spatial branch&bound for nonlinear constraints. In the sequel, we consider two versions of the nonlinear MIP, one as stated in (2.9) and the second one with outer convexification formulation as in (4.1). We consider again the option to include additional constraints for switching times. Since the problem has nonlinear constraints and integer variables and is highly combinatorially interconnected, it is extremely hard to solve.

As shown in Table 6.3, the solver is often not able to find any feasible solution within an hour, if we do not provide a solution in the beginning. And even, if the solver finds solutions by itself, in none of the cases, the primal bound exceeds the

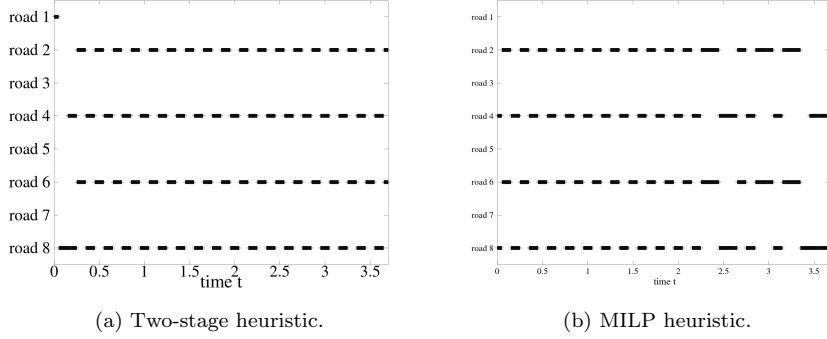


Figure 6.7: The black bars denote the green phases of the corresponding traffic light.

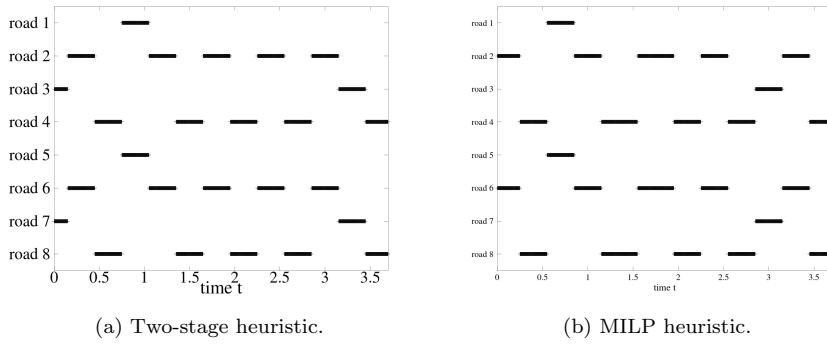


Figure 6.8: Heuristic solution considering bounds on switching times. The black bars denote the green phases of the corresponding traffic light.

heuristic solution found by the two-stage method, which in most of the cases obtains the solution much faster than in one hour.

When we provide the two-stage solution as incumbent for a warm start, SCIP is in none of the cases able to improve this primal bound within the first hour.

Another observation is, that the POC-formulation seemingly leads to a slightly faster decrease of the dual bound. Hence, the duality gap after one hour is in most cases better as in the original problem formulation (2.9).

**7. Conclusion.** For the traffic light optimization problem in [9], we proposed a solution heuristic consisting of five steps: Discretization, smoothing, solving a relaxed POC NLP with dynamic constraints (Stage I), reconstruction of a feasible mixed-integer solution from the CIAP MILP without dynamic constraints (Stage II), and, finally, a forward simulation to obtain a feasible solution candidate for the original problem. We prove a discrete approximation lemma that yields bounds on the quality of the Stage II solution with respect to the optimal CIAP objective function and some constants, which are independent of the time grid, but dependent on the spatial

POC	swt bnds	start	initial OFV	best OFV after 1h	dual bound after 1h	gap
2x2-junction coarse grid ( $\Delta t = 0.1$ , 2369 variables)						
no	no	cold	–	3.6255	3.8172	5.29%
		warm	3.6582	3.6582	3.8262	4.59%
yes	yes	cold	–	3.5997	3.7829	5.09
		warm	3.6118	3.6118	3.8873	7.63%
	no	cold	–	3.6451	3.7622	3.21%
		warm	3.6582	3.6582	4.0421	10.49%
	yes	cold	–	3.6036	3.7143	3.07%
		warm	3.6118	3.6118	3.6817	1.94%
2x2-junction fine grid ( $\Delta t = 0.05$ , 7929 variables)						
no	no	cold	–	3.1937	3.7583	17.68%
		warm	3.4020	3.4020	3.7498	10.22%
yes	yes	cold	–	–	3.6759	$+\infty$
		warm	3.3375	3.3375	3.6680	9.90%
	no	cold	–	2.8932	3.6022	24.50%
		warm	3.4020	3.4020	3.6068	6.02%
	yes	cold	–	–	3.5181	$+\infty$
		warm	3.3375	3.3375	3.5242	5.59%
8x4-junction coarse grid ( $\Delta t = 0.1$ , 10601 variables)						
no	no	cold	–	8.9689	21.4075	138.69%
		warm	20.7657	20.7657	21.5964	4.00%
yes	yes	cold	–	–	21.5065	$+\infty$
		warm	20.3205	20.3205	21.5678	6.14%
	no	cold	–	–	21.3149	$+\infty$
		warm	20.7657	20.7657	21.2885	2.52%
	yes	cold	–	–	21.7347	$+\infty$
		warm	20.3205	20.3205	21.3367	5.00%
8x4-junction fine grid ( $\Delta t = 0.05$ , 33313 variables)						
no	no	cold	–	7.1245	19.7777	177.59%
		warm	18.7817	18.7817	19.7772	5.30%
yes	yes	cold	–	–	19.7772	$+\infty$
		warm	18.1359	18.1359	19.7772	9.05%
	no	cold	–	–	19.2470	$+\infty$
		warm	18.7817	18.7817	19.2470	2.48%
	yes	cold	–	–	19.1891	$+\infty$
		warm	18.1359	18.1359	19.1874	5.80%

Table 6.3: Optimization via SCIP.

grid. Numerical results indicate that the obtained solution candidates cannot be improved by global state-of-the art MINLP methods within a reasonable amount of time. Furthermore, the two-stage solution candidates are better and usually faster to compute compared to global optima of piecewise linearized traffic flow models.

## REFERENCES

- [1] T. ACHTERBERG, *SCIP: Solving constraint integer programs*, Mathematical Programming Computation, 1 (2009), pp. 1–41.
- [2] E. BALAS, *Disjunctive programming and a hierarchy of relaxations for discrete optimization problems*, SIAM J. Algebra. Discr., 6 (1985), pp. 466–486.
- [3] G. M. COCLITE, M. GARAVELLO, AND B. PICCOLI, *Traffic flow on a road network*, SIAM J. Math. Anal., 36 (2005), pp. 1862–1886.
- [4] B. COLSON, P. MARCOTTE, AND G. SAVARD, *An overview of bilevel optimization*, Annals of Operations Research, 153 (2007), pp. 235–256.
- [5] IBM ILOG CPLEX, *IBM Deutschland GmbH, 71137 Ehningen*. Information available at <http://www-03.ibm.com/software/products/de/ibmilogcpleoptistud/>; visited on August 2015.
- [6] S. DEMPE, *Bilevel programming*, in Essays and Surveys in Global Optimization, Charles Audet, Pierre Hansen, and Gilles Savard, eds., Springer US, 2005, pp. 165–193.
- [7] G. FLÖTTERÖD AND J. ROHDE, *Operational macroscopic modeling of complex urban road intersections*, Transportation Research Part B: Methodological, 45 (2011), pp. 903 – 922.
- [8] M. GERDTS, *A variable time transformation method for mixed-integer optimal control problems*, Optimal Control Applications and Methods, 27 (2006), pp. 169–182.
- [9] S. GÖTTLICH, M. HERTY, AND U. ZIEGLER, *Modeling and optimizing traffic light settings in road networks*, Comput. Oper. Res., 55 (2015), pp. 36–51.
- [10] F. M. HANTE, *Relaxation Methods for Hyperbolic PDE Mixed-Integer Optimal Control Problems*, ArXiv e-prints, (2015). <http://arxiv.org/abs/1509.04052>.
- [11] F. M. HANTE AND S. SAGER, *Relaxation methods for mixed-integer optimal control of partial differential equations*, Computational Optimization and Applications, 55 (2013), pp. 197–225.
- [12] M. JUNG, *Relaxations and Approximations for Mixed-Integer Optimal Control*, PhD thesis, University Heidelberg, 2013.
- [13] M. JUNG, C. KIRCHES, AND S. SAGER, *On Perspective Functions and Vanishing Constraints in Mixed-Integer Nonlinear Optimal Control*, in Facets of Combinatorial Optimization – Festschrift for Martin Grötschel, M. Jünger and G. Reinelt, eds., Springer Berlin Heidelberg, 2013, pp. 387–417.
- [14] M. JUNG, G. REINELT, AND S. SAGER, *The Lagrangian Relaxation for the Combinatorial Integral Approximation Problem*, Optimization Methods and Software, (2014).
- [15] M. N. JUNG, G. REINELT, AND S. SAGER, *The Lagrangian relaxation for the combinatorial integral approximation problem*, Optim. Method. Softw., 30 (2015), pp. 54–80.
- [16] C. KIRCHES, S. SAGER, H.G. BOCK, AND J.P. SCHLÖDER, *Time-optimal control of automobile test drives with gear shifts*, Optimal Control Applications and Methods, 31 (2010), pp. 137–153.
- [17] T. KOCH, *Rapid Mathematical Prototyping*, PhD thesis, Technische Universität Berlin, 2004.
- [18] M. J. LIGHTHILL AND G. B. WHITHAM, *On kinematic waves. II. a theory of traffic flow on long crowded roads*, Proceedings of the Royal Society of London A: Mathematical, Physical and Engineering Sciences, 229 (1955), pp. 317–345.
- [19] P. I. RICHARDS, *Shock waves on the highway*, Operations Research, 4 (1956), pp. 42–51.
- [20] S. SAGER, H. G. BOCK, AND M. DIEHL, *The Integer Approximation Error in Mixed-Integer Optimal Control*, Math. Prog. A, 133 (2012), pp. 1–23.
- [21] S. SAGER, M. JUNG, AND C. KIRCHES, *Combinatorial integral approximation*, Math. Method. Oper. Res., 73 (2011), pp. 363–380.
- [22] SCIP, *Zuse Institute Berlin (ZIB)*. Information available at <http://scip.zib.de/>; visited on August 2015.
- [23] J. STOER AND R. BULIRSCH, *Introduction to numerical analysis*, no. 12 in Texts in applied mathematics, Springer, 2008.
- [24] A. WÄCHTER AND L. T. BIEGLER, *On the implementation of a primal-dual interior point filter line search algorithm for large-scale nonlinear programming*, Math. Progr., 106 (2006), pp. 25–57.
- [25] R. WUNDERLING, *Paralleler und objektorientierter Simplex-Algorithmus*, PhD thesis, Technische Universität Berlin, 1996. <http://www.zib.de/Publications/abstracts/TR-96-09/>.